SAND2016-6218J

MEMS Switching of Contour-Mode Aluminum Nitride Resonators for Switchable and Reconfigurable Radio Frequency Filters

Christopher D. Nordquist[1], Darren W. Branch[1], Tammy Pluym[1], Sukwon Choi[2], Janet H. Nguyen[3], Alejandro Grine[1], Christopher W. Dyck[1], Sean M. Scott[4], Molly N. Sing[5], and Roy H. Olsson III[1]
[1]Sandia National Laboratories, Albuquerque, NM, 87185, USA
[2]Department of Mechanical Engineering, The Pennsylvania State University, University Park, PA, 16802, USA
[3]RF Technology Group, MIT Lincoln Laboratory, Lexington, MA, 02420, USA
[4]Landauer, Glenwood, IL, 60425, USA
[5]Texas Instruments, Plano, TX, 75023, USA
E-mail: cdnordq@sandia.gov

Abstract –Switching of transducer coupling in aluminum nitride contour-mode resonators provides an enabling technology for future tunable and reconfigurable filters for multi-function RF systems. By using MEMS capacitive switches to realize the transducer electrode fingers, coupling between the metal electrode finger and the piezoelectric material is modulated to change the response of the device. On/off switched width extensional resonators with an area of <0.2 mm^2 demonstrate a Q of 2000, K^2 of 0.72, and >24 dB switching ratio at a resonator center frequency of 635 MHz. Other device examples include a 63 MHz resonator with switchable impedance and a 470 MHz resonator with 127 kHz of fine center frequency tuning accomplished by mass loading of the resonator with the MEMS switches.
Keywords – Reconfigurable filters, piezoelectric transducers, radiofrequency microelectromechanical systems, aluminum nitride resonators

1. Introduction

Achieving the reconfigurability and tuning range that has been demonstrated by electronic or electromagnetic filters with high-Q piezoelectric filters will improve the size, weight, and power of future radio frequency (RF) sub-systems such as receivers, transmitters, and signal processing units. In this work, we explore the opportunity for using MEMS switching to change the electrical coupling of transducer fingers to a contour-mode resonator, enabling programmable acoustic filter elements as building blocks for future reconfigurable filters. By extending previous efforts in MEMS capacitive switches and contour-mode acoustic resonators, switched transducers for contour-mode piezoelectric resonators are achieved. These switched transducers enable on/off switching of resonators as well as the opportunity to form frequency- and bandwidth-reconfigurable filters by increasing the number of electrode fingers and addressing these fingers separately to achieve programmed transfer functions.

The purpose of this work is to realize a miniature reconfigurable filter technology with high Q and miniature size. This capability would allow a single reconfigurable filter to replace multiple filters in an RF system, enhancing RF system performance while lowering overall system size, weight, power, and cost. If matured, it can be used to realize a wide range of filters with potential applications throughout the wireless communication, radar, and sensing industries.

1.1. Motivation and Previously Reported Work

Filters with adaptive properties such as tunable center frequency and variable bandwidth are key enablers for future multi-function, cognitive, and adaptive RF systems [1]. Due to potential benefits such as resistance to interference, adaptability to changing standards, and increased spectrum utilization, adaptive electromagnetic filters using electrical tuning by changing loading impedances with MEMS or solid-state devices have been an active area of research, with many excellent results reported to date [2]. While these types of filters have demonstrated excellent center frequency and bandwidth tuning, the selectivity and minimum bandwidth of these filters are limited by the relatively low Q of <1000 for available miniature electromagnetic resonators.

To achieve higher selectivity in a small volume, piezoelectric RF resonators such as Bulk Acoustic

Wave (BAW) devices, Surface Acoustic Wave (SAW) devices, and Contour Mode Resonators (CMR) exploit the high Q and small wavelength of acoustic wave propagation [3]. Filters using these types of resonators have become ubiquitous in RF front ends and signal processing systems. Because the acoustic resonance is defined by physical dimensions, real-time tuning of the filter properties such as center frequency or bandwidth has been limited to small effects such as thermal tuning [4] or electrical loading [5,6]. Currently, frequency tuning beyond a fraction of a filter bandwidth is only achievable by using electronic or MEMS switches to select pre-determined filters within a circuit [7]. Ferroelectric materials such as barium strontium titanate (BST) have been used to demonstrate switching by tuning of the acoustic sound velocity, but have limited Q, high capacitance, and present materials integration challenges [8,9]. As a result, there are currently no known practical approaches for realizing reconfigurable piezoelectric resonators or filters [10].

Prior to this work, limited switching of the coupling of acoustic microresonators had been proposed and described. Electromechanical transduction of fingers that are not physically attached to the substrate has been used for non-destructive characterization of piezoelectric substrates by a test apparatus in which transducer fingers are pressed into contact with the substrate surface to excite a SAW mode [11]. At the microscale, an electrostatically transduced microresonator was reported to achieve an on/off ratio of 15 dB and a Q of 8,800 by using an electrostatic force to close the actuation gap and turn off the resonator by damping the Q [12], and the approach was also used for frequency tuning of 5300 ppm by adjusting the electrode gap [13]. However, the airgap in the on-state causes low coupling and high motional impedance, and the capacitance in the off-state results in high off-state capacitance which presents a load to the circuit. Another proposed approach is a movable upper electrode on a BAW device for a switched device response [14], with limited opportunities for broad reconfigurability because the resonance is determined by the film thickness. Also, using electronic switches to select sets of transducer fingers has been used to program the response of a SAW device [15], but the disconnected metal fingers remained in contact with the piezoelectric material and contributed parasitic capacitance that limits performance in a filter element. We previously reported this MEMS switched-finger approach to realize on/off two-finger resonators, but the Q was limited to approximately 400 by damping losses where the switch beam crossed the etched edge of the AlN membrane [16]. While these initial results were promising, the demonstrated resonators did not match the performance of a fixed device, which has a Q>1000 and coupling that allows practical impedance matching to 50 Ω. The devices reported in this paper represent a substantial advance over these previously reported results.

1.2. Reconfigurable RF Filter Approaches

Four approaches are proposed for applying this technology towards reconfigurable RF filters and similar devices. These approaches are sketched as device cross-sections in figure 1, and use MEMS switching to vary the response of either the transducer or reflector elements and change the device response. The transducer fingers convert applied RF signals from the electrical to the mechanical domain and launch an RF acoustic wave into the structure at the input; the inverse process converts acoustic signals to electrical signals at the output. The placement of the transducer electrode fingers determines the response of the device as a function of frequency, and fingers can be turned “on” and “off” by bringing them into and out of contact with the substrate.

To support resonance, the devices must have reflectors that define a resonant cavity containing the acoustic wave. These reflectors may be realized with etched sidewalls or with Bragg reflectors, which are periodic arrays of metallic electrode fingers that are grounded and reflect the acoustic signal when the electrode finger width and spacing each correspond to a quarter wavelength (λ/4) [17]. These reflector fingers may be realized using the same electrode technology as the input and output transducers.

The basic electrode switching approach, shown in figure 1(a), switches the electrode fingers into and out of contact with the piezoelectric material of a resonator. Moving the electrodes into contact with the piezoelectric material maximizes the electric field and coupling to the acoustic mode, while separating the electrode from the piezoelectric material minimizes coupling. The selected acoustic mode is determined by the lateral location of the fingers relative to each other and the end reflectors of the device. In this way, the resonator can be switched between on- and off-states by moving the electrodes into and out of contact.

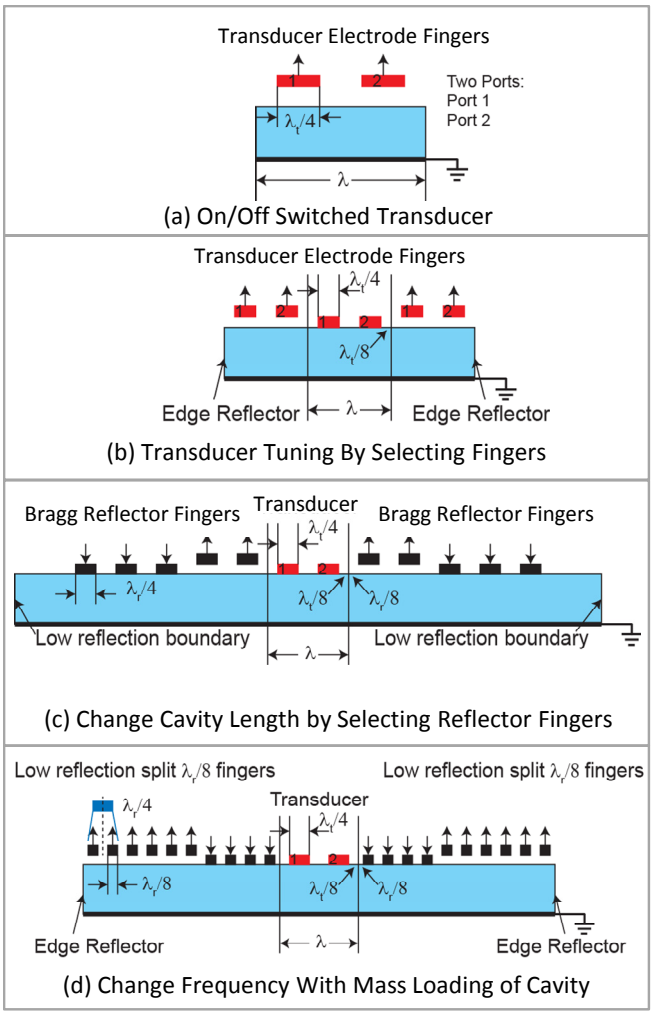

Figure 1. Four proposed methods of realizing switchable and reconfigurable RF resonators using different configurations of moveable electrode fingers wired as transducers and reflectors. Each finger has variable separation between the metallic electrode and the piezoelectric material, which changes the electromechanical coupling between the electrode finger and the device.

Independent actuation of the transducer fingers, as shown in figure 1(b), may be used to access different acoustic modes of a resonator and change the resonant frequency of the device. This should allow reconfigurability across a broad range frequencies, with smaller fingers and pitches allowing the selection of a higher number of acoustic modes.

Another approach to achieving coarse frequency tuning is to use the MEMS fingers to realize a Bragg reflector, as shown in figure 1(c). Fingers can be moved into and out of contact with the resonator to change the effective length of the resonant cavity, thereby changing the resonant frequency. This approach requires good mechanical contact of the reflector finger with the piezoelectric material to ensure a large change in mechanical impedance for the reflector.

To achieve fine tuning, MEMS switched fingers may be used to load acoustic propagation regions and lower the acoustic propagation velocity in the structure, as shown in figure 1(d). Fingers that are λ/8 wide on a λ/4 pitch can be used to minimize reflection from the electrodes while providing mass loading. This can be used in conjunction with the other approaches to fine-tune the center frequency of a resonator or to tune the acoustic phase, and thus coupling, between two device sections.

The remainder of this paper will introduce the switch properties and then focus on the switched electrode finger technology and demonstrations of the on/off switched transducer, transducers with switched numbers of fingers, and resonance tuning through mass loading. These results demonstrate the potential capability of this approach for reconfigurable and tunable filters.

2. MEMS Switching of Transducer Fingers

2.1. MEMS Switch Description

The fabrication process used to realize these switches is a combination of an AlN contour-mode resonator process and a capacitive switch process using a shared release. This process has been summarized previously [16], and will be reported in more detail separately [18]. A simplified cross-section of a MEMS capacitive switch with side pull-down electrodes is shown in figure 2. The switch serves as the piezoelectric transducer electrode finger and consists of a 0.2 µm-thick fixed-fixed AlCu beam that is suspended approximately 1 µm above the AlN (0.75 µm or 1.5 µm thick) surface when open and is pulled into contact with the AlN when closed. The switch fingers are anchored at each end of the beam outside of the active resonator area to create a fixed-fixed beam. The switch beam is reinforced with a 1 µm-thick AlCu layer in the region outside of the device aperture, with a 4 µm-long thin section near the anchor serving as a flexure to lower the pull-in voltage of the switch. Because intimate contact between the switch and AlN is critical, deformation is minimized by using fixed-fixed structures and fabricating the structures from tensile films with low stress gradient.

The switch shown in figure 2 is actuated by applying a positive voltage to the bridge and a negative voltage to the actuation electrode while

grounding the bottom electrode of the resonator. The use of separate actuation electrodes allows for the selection of individual switch fingers, while the bridge bias provides electrostatic force to ensure good contact with the AlN film. In versions of the switch where individual finger control is not required, the actuation electrode is also grounded and pull-down was achieved by biasing only the bridge.

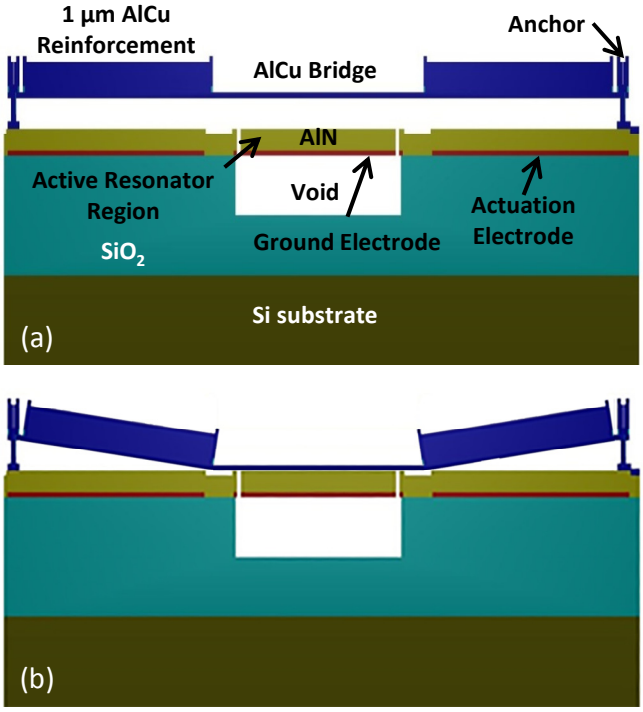

Figure 2. Cross-section drawing of a typical MEMS-switched transducer finger with separate actuation electrodes at the edges in the (a) up and (b) down states.

2.2. Switch Coupling Model

The coupling of the electrode finger to the piezoelectric film is critical for the switched resonator to achieve performance similar to that of a fixed resonator. This coupling may be degraded by incomplete contact caused by unintended deformation or curvature in the AlN membrane or switch beam, or by surface roughness at the contacting interface. The switching range and required contact of the switch was predicted using Comsol Multiphysics (Comsol Inc., Burlington, MA) finite element modeling (FEM) while the resonator response in the up and down states was predicted using coupling-of-modes (COM) modeling [19]. As seen in figure 3, the electrical coupling between the finger and the piezoelectric film decreases by 10% for a gap of 10 nm and by 97% for a gap of 2000 nm when compared to the transduction of an intimately attached finger. Thus, assuming that the average switch gap due to roughness and deformation is 10 nm, down-state fingers represent a 10% reduction in coupling when compared to the ideal device, and for a 1 µm gap the ratio of coupling between the up- and down-states is expected to be a factor of 14. Higher roughness or curvature in the switch or AlN will degrade this on/off ratio, resulting in lower piezoelectric coupling while in the on-state and a higher off-state capacitance for a given on-state impedance.

This approach also provided a means to investigate the impact of unintended variation of the gap thickness due to surface roughness or curvature, which was approximated using a 5th order polynomial. The admittance of a finger with a uniform gap across the aperture was nearly identical to the case where the gap varied spatially, so imperfect contact due to surface roughness or distortion may be approximated by a small uniform gap. Therefore, the mean gap distance was taken as an effective parameter in the 2D FEM simulations.

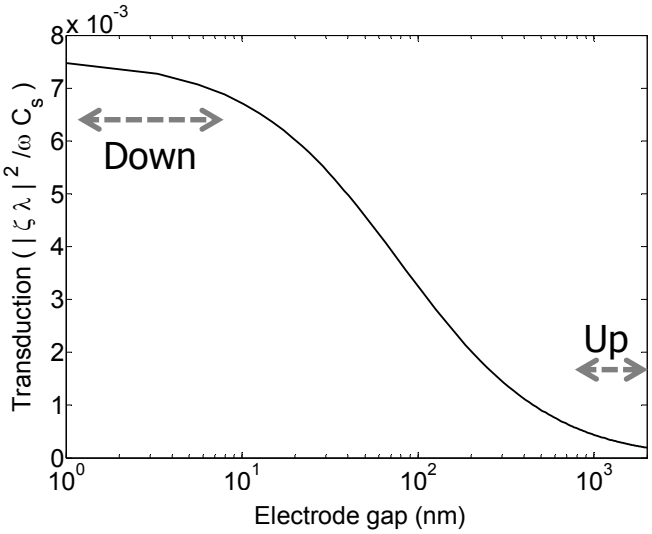

Figure 3. Finite element modeled transduction of an electrode finger as a function of height above the top surface of a 0.75 µm-thick AlN film.

2.3. Measured Switch Coupling

The measured transmission (S_{21}) for a series-connected switch between the bridge and the lower electrode (across the AlN) is shown for a fabricated-down switch, a switch in the up-state, and a switch in the down-state in figure 4. The switches were tested using GSG100 probes with an Agilent 5071 network analyzer that was calibrated at the probe tips, and the measurements include the 5 fF of series capacitance

from the test pad structure. A bias tee was used to introduce a voltage difference between the bridge beam and bottom electrode, generating an electrostatic force that pulled the switch bridge into contact with the AlN surface. This particular switch closed when the bridge voltage was >20 V, but was tested at 50 V because a higher voltage increases the downstate capacitance by pulling the switch electrode into better contact with the AlN material. The tested switch has a total length of 350 µm, bridge width of 20 µm, a bridge height of 1 µm, AlN thickness of 0.75 µm, and an overlap area of 1,800 µm^2. After subtracting the 5 fF from the test pads and assuming zero fringing capacitance, the up-state capacitance density is 14 aF/µm^2, the down-state capacitance is 117 aF/µm^2, and the fixed-down capacitance is 136 aF/µm^2. The 15% reduction in down-state capacitance ratio suggests an equivalent gap of ~30 nm between the finger and the AlN dielectric. The on/off ratio of 10 is lower than predicted by the model due to this down-state gap and fringing capacitance, but is adequate for piezoelectric switching.

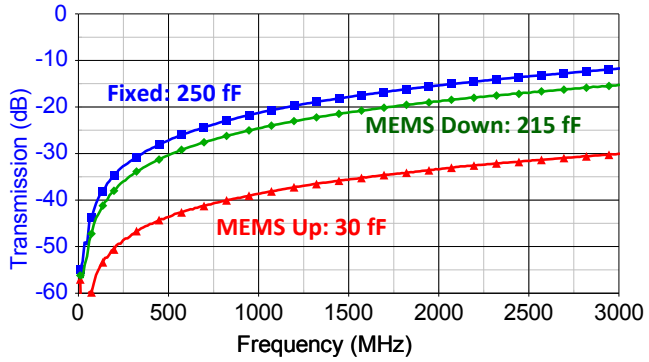

Figure 4. Measured transmission between the bridge and bottom electrode of an AlN capacitive switch in the fixed (fabricated down), up-, and down- states. The equivalent capacitance value shown includes 5 fF from the device pads.

3. On/Off Switched Resonator

3.1. Device Structure

The switched contour-mode resonator design, shown with four fingers in the 3D model in figure 5, uses quarter-wavelength fingers on a half-wavelength pitch to excite the appropriate overtone of the AlN membrane. The input and output ports are connected to alternating fingers, creating an interdigitated electrode structure.

The fingers are 4 µm wide, corresponding to one quarter of an acoustic wavelength, and are placed on a pitch of 8 µm, corresponding to half of an acoustic wavelength. Energy is confined to the resonator by sidewalls that are etched through the AlN membrane parallel to the fingers. The expected AlN acoustic velocity of 10,400 m/sec results in a center resonant frequency of 650 MHz prior to loading from metal electrode fingers. A continuous Ti/TiN/AlCu electrode underneath the AlN is grounded to provide a ground electrode for d_{31} piezoelectric transduction as well as an actuation ground for the MEMS switches.

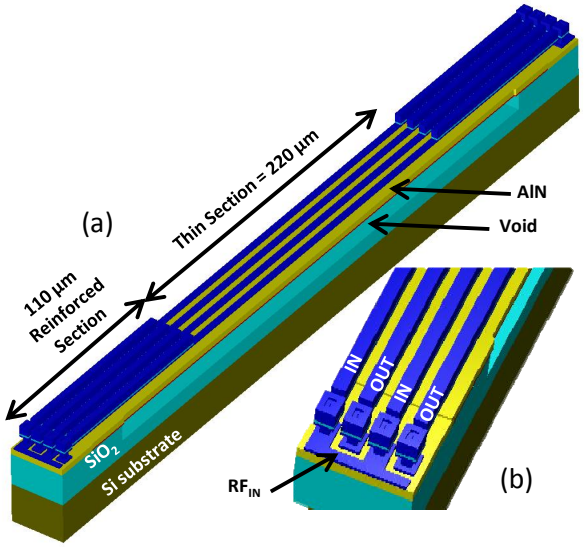

Figure 5. A 3-dimensional model of a 4-finger switched width extensional resonator. (a) The entire structure spanning the length of the switches. (b) Detail of the anchor region and routing of the RF signals to the switch fingers.

A six-finger switched resonator is shown in the optical image in figure 6(a), which also shows the fixed resonator on which the design is based in figure 6(b). The fixed width-extensional resonators provide a comparison to a resonator which has been used previously to demonstrate three- and four- pole filters operating near 500 MHz with 50 Ω impedance [20]. The devices reported here do not a use a SiO_2 temperature compensation layer, resulting in a higher frequency of 635 MHz for the same dimensions.

The switches used in the on/off resonator have a continuous ground plane underneath the resonator and switches, with no separate actuation electrodes at the edge of the switch. All of the switches are actuated simultaneously by applying a voltage to the bridges through the RF input and output electrodes using a bias tee while the bottom metal electrode is held at ground. Typical switch pull-in voltages are 20 V, while most testing was performed with switch biases

of 50 V to ensure good contact between the switch electrode and AlN.

The switch beam has a total length of 450 µm, with a 220 µm-long, 0.2 µm-thick section in the center and a 1.0 µm-thick reinforced section on each end designed to prevent pull-in of the outer portion of the beam so that the device active aperture is limited to the thinner central portion of the beam that is expected to be in contact with the aluminum nitride material. The intended device aperture is 220 µm, or 14 wavelengths, wide. Details of the anchor and reinforcement are shown in the scanning electron microscope image in figure 7.

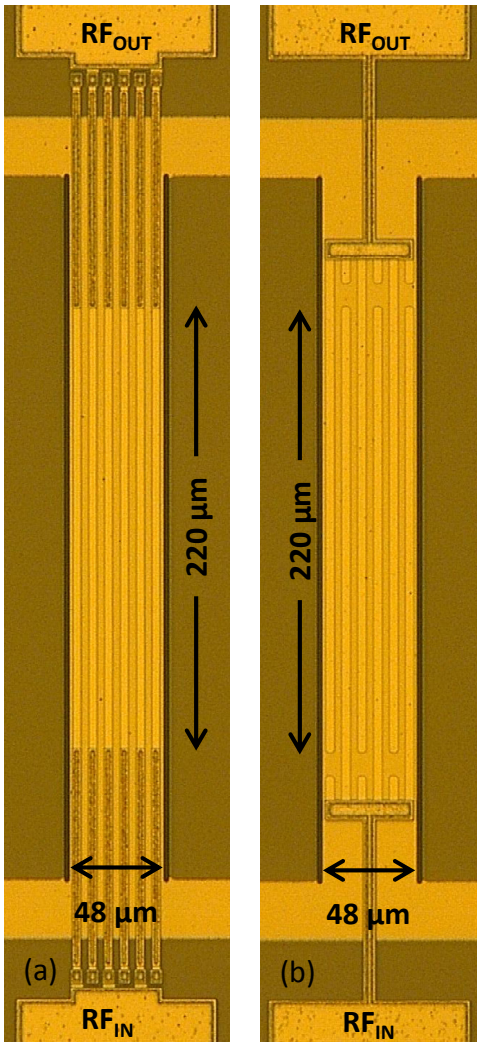

Figure 6. Optical micrographs of 6-finger (a) switched and (b) fixed resonators.

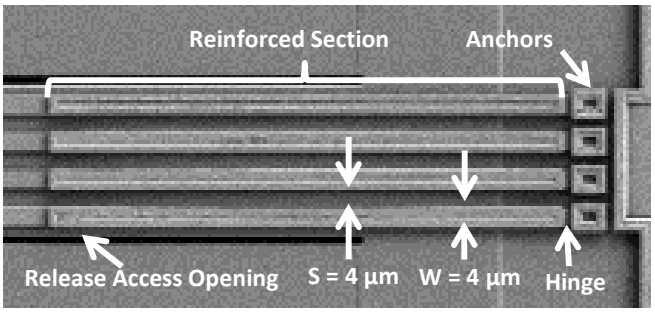

Figure 7. Scanning electron microscope image of the anchor and reinforcement region of the switch for a four-finger switched resonator.

3.2. Measured Response vs. Actuation Voltage

An array of resonators with the number of fingers ranging from 2 to 16 were fabricated and tested using on-wafer probing as described previously for the switches. Fixed and switched resonators were fabricated on the same wafer with a 1.5 µm-thick AlN layer to provide a comparison of device properties. The switched devices, such as the six-finger device shown in figure 6(a), use the MEMS switches to realize the transducer fingers, and are switched by applying a DC actuation voltage between the switch beam and the ground electrode. Fixed resonators used the standard design with the fingers intimately bonded to the AlN and tied together with a single bus on the resonator as shown for a 6-finger device in figure 6(b).

The measured and equivalent circuit model transmission responses of a switched 6-finger resonator at bias voltages of 0 V and 50 V, along with results from a fixed resonator of the same dimensions, are shown in figure 8 and summarized in table 1. The resonant peak of the switched device in the up-state (V_{bridge} = 0 V) is -31.5 dB at 638.2 MHz, slightly above the capacitive feedthrough of -42 dB. At a bridge voltage of 50 V, the switches have pulled into contact with the AlN and the transmission increases to -7.3 dB at 635.6 MHz. The loaded Q of the switched resonator at 50 V is 1350 and the unloaded Q is 2000, similar to the Q of the fixed down resonator with the same number of fingers. This 24 dB increase in transmission shows the change in piezoelectric modulation enabled by the contact and separation of the switched finger.

The transmission peak through the fixed device is -3.4 dB at 643.3 MHz, about 4 dB higher than the switched device. This is due to better contact with the intimately attached fingers of the fixed device, compared with the non-ideal contact of the

electrostatically actuated switch on the AlN surface with ~30 nm surface roughness. The out-of-band rejection of the fixed device is higher than that of the switched device because of lower coupling capacitance of the fixed electrode compared to the switched electrodes, in which the switches have higher capacitance due to edge coupling along their entire length.

The switched resonator has spurious responses between the resonance and anti-resonance. The most likely cause of these resonances is leakage of the acoustic wave into the switch bus, but specific approaches to eliminate spurious modes from these switched devices have not been explored.

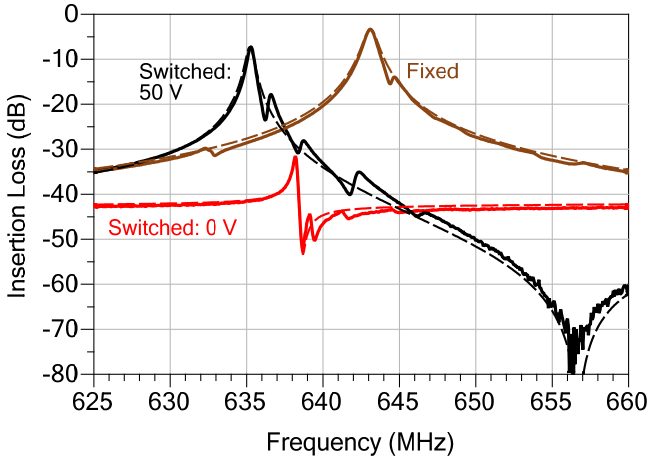

Figure 8. Measured insertion loss (solid line) and equivalent circuit model response (dashed line) of a switched six-finger resonator in the on- and off- state and a fixed six-finger resonator.

Table 1. Equivalent Circuit Parameters for the 6-Finger Fixed and Switched Resonators.

Parameter	Fixed	0 V	50 V
f_{res} (MHz)	643.4	638.2	635.6
Peak S_{21} (dB)	-3.4	-31.5	-7.3
Q_u	2150	2500	2000
$C_{shunt1,2}$ (fF)	375	85	260
$C_{parallel}$ (fF)	3	19	15
C_x (fF)	2.4	0.025	0.96
L_x (μH)	25.8	2490	65.4
R_x (Ω)	45	4000	130
K^2 (%)	1.3	0.06	0.72

3.3. Equivalent Circuit Parameters

The equivalent electrical circuit for the fixed and switched resonators and the governing equations for the motional inductance, capacitance, and resistance as a function of the center frequency f_{res}, quality factor Q, and coupling coefficient K^2 are shown in figure 9 [21]. The equivalent circuit parameters for fixed and switched resonators in the on- and off- states are shown in table 1. The shunt capacitance C_{shunt} was determined by curve fitting the magnitude and phase of S_{11}. The center frequency f_{res}, Q_u, and motional resistance R_x were determined by curve fitting to the magnitude and phase of S_{11} and S_{21}. These extracted parameters were then used to calculate the motional capacitance C_x, motional inductance L_x, and coupling K^2 using the equations shown in figure 9.

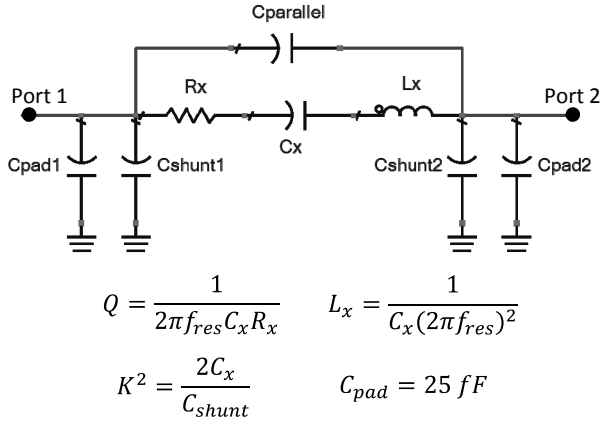

Figure 9. Resonator equivalent circuit model and equations.

The equivalent circuit parameters provide insight into the operation of the device. The frequency of the switched resonator in the on-state is 1.2% lower than the frequency of the fixed device due to the additional mass from the bridge touching the surface of the resonator loading the AlN and lowering the acoustic velocity. Additionally, the frequency of the switched device decreases slightly as the bridge is brought into contact with the surface and slightly loads the device. The unloaded Q is 2000 for the switched-on device and 2150 for the fixed device, but is 2500 for the up-state device because the fingers are not in contact and damping the resonator.

The measured shunt capacitance to ground includes approximately 25 fF of capacitance from the pad, which is accounted for in the model as C_{pad}. The capacitance of the feeds and bridge from the test pad to the center of the device are considered part of the resonator and included in the equivalent circuit parameter C_{shunt}. The device shunt capacitance is

higher for the fixed resonator because all of the trace from the pad to the active device area is in intimate contact with the AlN, while the switched resonator has portions of the feeds that are not in contact with the AlN film. The shunt capacitance of the switched resonator starts at 85 fF for the up-state bridge and jumps to 260 fF when all of the bridges are in contact.

The parallel capacitance ($C_{parallel}$) is much higher for the switched resonator than the standard resonator because of the edge coupling along the length of the suspended bridges. This parallel capacitance drops slightly as the bridge is brought into contact because more of the electric field is terminated at the ground plane as the bridges draw closer to the AlN layer. This 14 fF of parallel capacitance is the source of the anti-resonance that is present in the switched resonator but not in the fixed resonator.

These results show that the switching can be considered and modeled as a change in K^2 and C_{shunt} while maintaining device Q and center frequency. As seen in Table 1, the coupling K^2 increases as the switch closes due to the increasing contact of the bridge to the AlN piezoelectric material, increasing the motional capacitance and reducing the motional resistance. The motional inductance decreases proportionally to the increase in the motional capacitance because the resonant frequency is constant.

3.4. Intermodulation Distortion

Intermodulation distortion of a six-finger resonator was tested using a two-tone measurement with both tones in the resonator passband and separated in frequency by 0.1 MHz. The response of a switched resonator is compared to that of a fixed resonator at -20 dBm input power and +8 dBm input power in figure 10. With -20 dBm input, neither resonator generates intermodulation products above the noise floor, while at +8 dBm significant modulation products are present and of similar magnitude for both the switched and fixed devices.

The plot of the power in the fundamental tones and third-order tones as a function of input power are shown in figure 11. Other than the slightly higher loss of the switched device, the device responses are similar. From the extrapolation of the third-order tones, the input-referred IP3 point is approximately +20 dBm and equal for both the switched and fixed devices, demonstrating that MEMS switching does not degrade the linearity of the resonator.

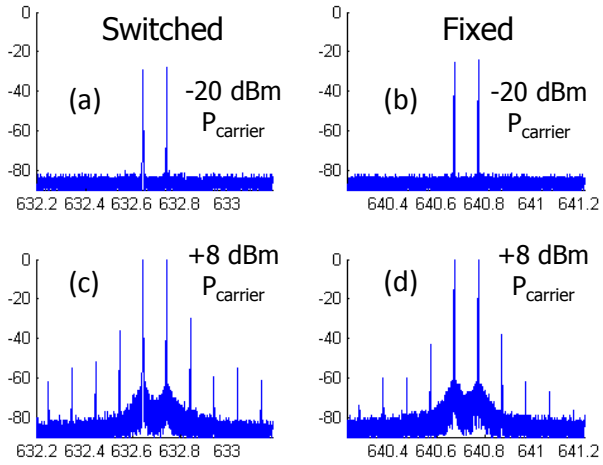

Figure 10. Output spectra of the switched (left) and fixed (right) six-finger devices when driven with two tones at -20 dBm (top) and +8 dBm (bottom) power. The tone separation is 0.1 MHz, and both tones are within the resonator passband

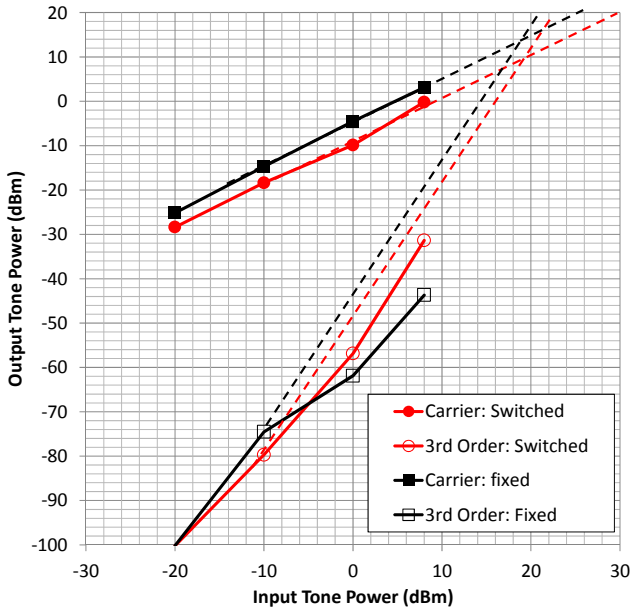

Figure 11. Input Power vs. Output Power of the fundamental and third-order tones during two-tone measurements of the switched and fixed resonators.

3.5. On/Off Resonator Coupling-of-Modes Model

Coupling-of-modes (COM) was used to predict and analyze the response of the switched resonator, and was chosen since it scalable for devices that have a large number of switchable fingers [19]. The COM parameters were extracted from 2D FEM simulations of a single period of the switch structure shown in figure 1(a) using several different finger-substrate gaps.

The parameters for the COM simulation were wavelength $\lambda = 16$ µm, $N_i = 3$ input electrodes, $N_o = 3$ output electrodes, aperture width = 14λ, and the mean gap was 60 nm. Several 2D FEM simulations were performed to determine the actual mean distance of a switched finger above the AlN substrate by comparing with measured static capacitance. The extracted COM parameters from the 2D FEM analysis were: (S0) $v = 10374.4$ m/s, $\kappa_{12}p = 0.016$, $|\zeta p|^2/\omega C_s = 0.0060$, $C_s = 204.8$ pF/p/m, $R_e = 3.2$ kΩ/m, $D = 0$, and $\gamma = 0.008$ dB/λ. To capture the parasitic effects of electrical pads, bussing, and feedthrough capacitance in the model, the COM results were inserted into an external circuit as shown in figure 12(a). The extracted phase velocity from the 2D FEM model predicted a higher resonant frequency than the measurement, which corresponded to a phase velocity difference of +2.5%, probably due to loading from the bottom metal. By adjusting for this small velocity shift in the COM model, the agreement with the measurement was excellent, as shown in figure 12(b).

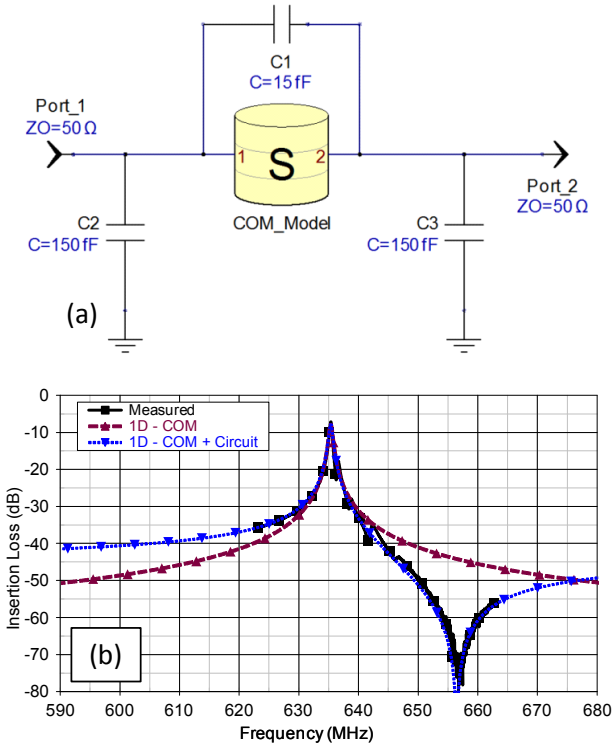

Figure 12. Match between the COM model and the measured data, a) external circuit, and b) insertion loss.

4. Switchable Resonant Impedance Transformer

The switchable resonant transformer uses switching of transducer fingers to change the number of fingers in contact and the impedance ratio of a resonant device. Fixed resonant transformers have been described in AlN and PZT tecnologies previously, and provide miniature on-wafer RF impedance transformation [22,23]. An optical image of the switched resonant transformer is shown in figure 13, and consists of two ports with three electrode fingers each on an AlN resonator with a width of 95 µm and an overall length of 165 µm, targeting a one-wavelength resonance of 63 MHz. The fingers are connected to the actuation electrodes so that, in addition to all of the switches in the up-state, three input/output finger combinations may be selected: 1:2, 2:1, 3:3. The bridge voltage is fixed at +5 V and the individual switches are actuated by setting the actuation pads to -20 V.

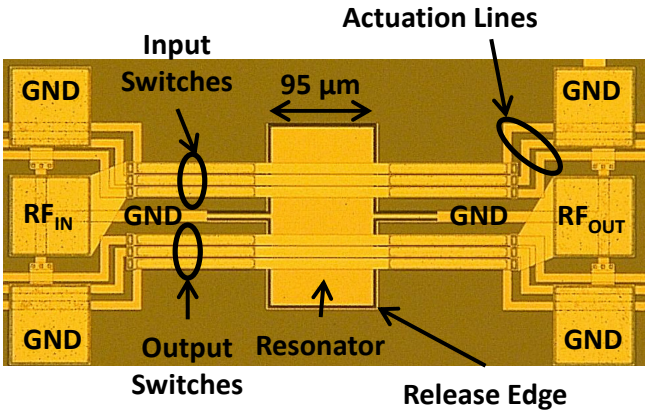

Figure 13. Optical microphotograph of the 63 MHz switched resonant impedance transformer with 3 fingers per transducer.

The insertion loss and the magnitude of the device input impedance (Z_{11}) for each port is shown in figure 14. The capacitance of the pad structure is 150 fF, which is subtracted from the measurement. The device has a loaded Q of 1500, but the insertion loss at resonance ranges from 40 dB to 55 dB because the device was sized for an impedance of approximately 5000 Ω but measured and plotted in a 50 Ω system. Lower impedances can be obtained with more device fingers and larger devices, but a small device was fabricated to ensure fabrication yield.

The device port impedance magnitude ranges from approximately 12 kΩ in the up-state to 5 kΩ when all of the fingers are down. When one finger is down at a port, the input impedance is approximately 7.5 kΩ, and when two fingers are down, the impedance is

approximately 6.5 kΩ. The port impedances switch values when the device is switched between the 1:2 and the 2:1 impedance states. The impedances of the two ports are slightly different due to differences in the switch contact between the two ports. With appropriate scaling of the device, reduction of parasitic shunt capacitance, and improvements in the coupling of the finger to the resonator, this approach may be used to realize practical tunable impedance transformers or on-chip programmable gain and attenuation stages.

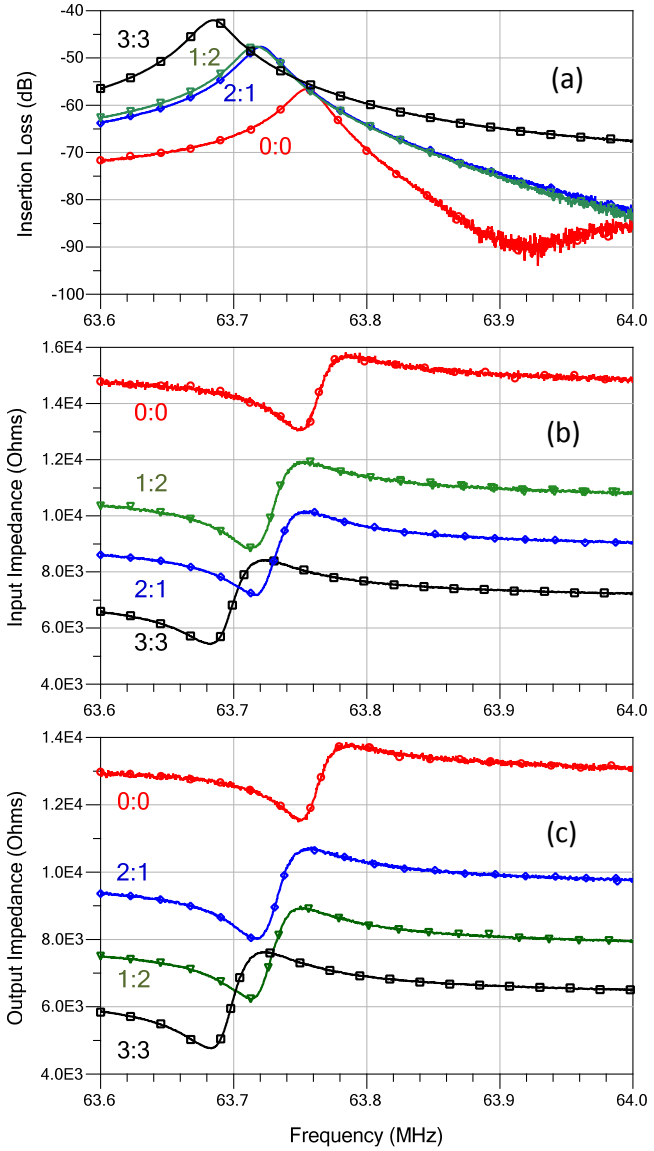

Figure 14. Measured response of the switched impedance transformer for the four tuning states: (a) Insertion loss in a 50 Ω system, (b) port 1 input impedance magnitude (Z_{11}), (c) port 2 input impedance magnitude (Z_{22}). The states are designated by the number of input and output fingers actuated as N_{in}:N_{out}.

5. Fine Resonator Tuning With Mass Loading

The fine-tuned resonator design uses mass loading to change the acoustic velocity within the resonator. This device, shown in figure 15, uses an eight-finger fixed interdigitated transducer on a 12 µm pitch within a resonant cavity formed by two sets of 20 Bragg reflector fingers on a 10 µm pitch for an unloaded center frequency of 477 MHz. The Bragg reflector provides a reflective boundary condition while still allowing for rigid mechanical support at the ends of the AlN device. Six 5 µm-wide fingers in the two spaces between either side of the transducer and each reflector are switched independently to provide mass loading.

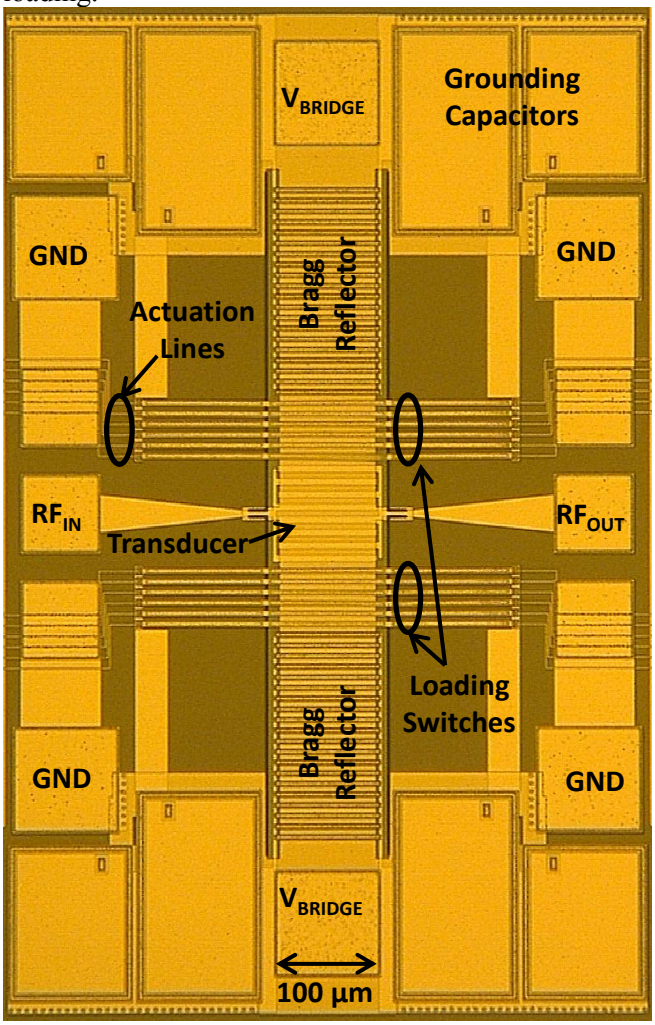

Figure 15. Optical photomicrograph of a device that uses fine-tuning to adjust the acoustic velocity within the resonator. This device uses fixed transducer fingers and Bragg reflectors, with mass loading achieved with switchable fingers between the transducer and each reflector.

The measured insertion loss of this resonator with 0 through 6 loading fingers applied to each side of the transducer is shown in figure 16. The resonator has a center frequency of 476.815 MHz and Q_L of 600 when unloaded, which changes to a center frequency of 476.688 MHz with similar Q when all of the fingers are actuated. This tuning is sufficient to fine-tune the position of the filter peak within a bandwidth. Each pair of fingers shifts the frequency downwards by 21.1 kHz, and larger frequency shifts may be obtainable with higher numbers of fingers over a longer distance.

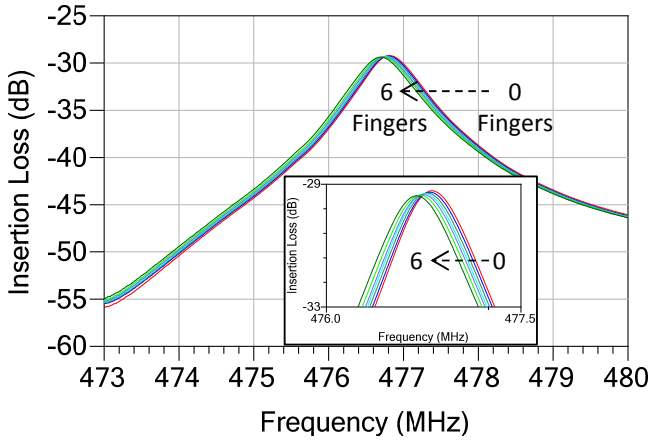

Figure 16. Fine-tuning of a resonator through mass loading by actuating between 0 and 6 fingers on each side of the transducer.

6. Future Work

While this work has demonstrated the functionality of the switched transducer concept, achieving the best possible performance from the technology will require optimization and additional progress in several areas. First, additional process iterations and improvements will be required to improve the yield, reproducibility, and reliability of the combined resonator/switch technology to that required for relevant reconfigurable RF microsystems. Second, additional design effort will allow more complex filters with improved performance in terms of loss, coupling, and tuning range. In this area, additional switched transducer designs and devices will be required to achieve reconfigurability over frequency ranges of an octave or greater, and switchable Bragg reflectors will be required to achieve tuning of acoustic cavity dimensions. Third, technology maturation will require additional testing over environmental conditions such as temperature and vibration. Finally, integration with packaging and control electronics will be required for this technology to gain acceptance for a wide range of applications.

An additional direction to explore is increasing the frequency and bandwidth to cover digital wireless communication bands at 1 GHz and beyond. In order to scale to the higher frequencies, the width of the quarter-wavelength fingers must be scaled from the current 4 μm for a frequency of 500 MHz down to 1 μm for 2 GHz, and to even smaller dimensions for higher frequencies. This can be achieved with modern microfabrication capabilities, but the higher aspect ratio of the switch will present mechanical and fabrication challenges in the switch itself, and the smaller dimensions will increase undesired electromagnetic coupling. The maximum filter bandwidth will be limited by the material coupling, so filter bandwidths beyond 0.3% will require applying this approach to higher bandwidth materials such as lithium niobate [24] or alloys of aluminum nitride that offer increased coupling [25]. With appropriate maturation and scaling, this technology has the potential to address tunable and reconfigurable filter needs for a large range of future applications.

7. Conclusions

MEMS switching of transducer fingers provides the opportunity to realize reconfigurable and switchable piezoelectric filters with broad tuning ranges as well as fine tuning. On/off resonators with Q>2000 at 635 MHz have been demonstrated, providing performance similar to a fixed resonator but with >20 dB of on/off ratio, proving that the MEMS-switched transducer finger has the potential to be used to realize reconfigurable high performance RF piezoelectric filters. In addition, a resonant device with switchable impedance was demonstrated, offering potential for miniature tunable resonant impedance transformers or matching networks. Finally, fine tuning was demonstrated by mass loading of a resonator to reduce the acoustic velocity and provide tuning within the bandwidth of a piezoelectric resonator. This demonstrates the potential of MEMS transducer switching of contour-mode resonators for realizing reconfigurable filters and other resonant devices.

Acknowledgments

This work was supported by the Laboratory Directed Research and Development (LDRD) program at Sandia National Laboratories and the DARPA RF

FPGA program. Sandia National Laboratories is a multi-program laboratory managed and operated by Sandia Corporation, a wholly owned subsidiary of Lockheed Martin Corporation, for the U.S. Department of Energy's National Nuclear Security Administration under contract DE-AC04-94AL85000. These devices were fabricated in the Sandia MESAFab, and the authors thank the MESAFab operations team for fabrication contributions. M. H. Ballance, A. Schiess, and G. Grossetete provided test and measurement support.

References

[1] Rais-Zadah M, Fox J T, Wentzloff D D and Gianchandani Y B 2015 Reconfigurable Radios: A Possible Solution to Reduce Entry Costs in Wireless Phones *Proc. IEEE* **103** 438–451

[2] Chappell W J, Naglich E J, Maxey C, and Guyette A C 2014 Putting the radio in 'Software-Defined Radio': Hardware developments for adaptable RF systems *Proc. IEEE* **102** 307–20

[3] Piazza G, Felmetsger V, Muralt P, Olsson R H and Ruby R 2012 Piezoelectric Aluminum Nitride Thin Films for Microelectromechanical Systems *MRS Bulletin* **37** 1051-61

[4] Kim B, Nguyen J, Wojciechkowski K E, and Olsson R H 2013 Oven-Based Thermally Tunable Aluminum Nitride Microresonators *J. Microelectromech. Sys.* **22**, 265-75

[5] Kim B, Olsson R H and Wojciechkowski K E 2011 Capacitive Frequency Tuning of AlN Micromechanical Resonators *Proc. Solid-State Sensors, Act. Microsys. Conf.,*502-5

[6] Warder P and Link 2015 Golden Age for Filter Design: Innovative and Proven Approaches for Acoustic Filter, Duplexer, and Multiplexer Design *IEEE Microwave Mag* **16** 60-72

[7] Crespin E R, Olsson R H, Wojciechowski K E, Branch D W, Clews P, Hurley R and Gutierrez J 2012 Fully Integrated Switchable Filter Banks *Proc. IEEE MTT-S Intl Microw. Symp,* DOI: 10.1109/MWSYM.2012.6259652

[8] Mansour A, Hmeda M, Kalkur T S, Alpay P, Sbockey N and Tompa G S 2015 Switchable Band Pass BAW Filter Based on $Ba_{0.7}Sr_{0.3}TiO_3$ for C Band RF Applications," *Proc. 2015 IEEE Intl. Symp. App. Ferroelectric. (ISAF)* 222-5

[9] Lee V, Lee S, Sis S A and Mortazawi A 2014 Switching Reliability of Baraium Strontium Titanate (BST) BAW Devices *Proc. 44th European Microwave Conf.* 500-3

[10] Aigner R 2015 Tunable Filters? Realty Check Foreseeable Trends in System Architecture for Tunable RF Filters *IEEE Microwave Mag* **16** 82-8

[11] Lewis M F and Patterson E 1971 Some properties of acoustic waves on Y-cut quartz *J. Acoustic Soc. America* **49** 1667-8

[12] Schneider R A and Nguyen C T-C 2014 On/Off Switchable High-Q Capacitive-Piezoelectric AlN Resonators," *Proc. 2014 IEEE Intl. Conf. MEMS,* 1265-8

[13] Schneider R A, Naing T L, Rocheleau T O and Nguyen C T-C 2015 Gap Reduction Based Frequency Tuning for AlN Capacitive-Piezoelectric Resonators *Proc. IEEE Freq. Cntl. Symp.,* 7000-5

[14] Pang W, Zhang H, Yu H and Kim E S 2004 Electrically Tunable and Switchable Film Bulk Acoustic Resonator *Proc. IEEE Intl. Freq. Cntl. Symp* 22-6

[15] Haartsen J C 1990 Development of a Monolithic, Programmable SAW Filter in Silicon *Proc. IEEE MTT-S International Microwave Symposium* 1115-8

[16] Nordquist C D, Olsson R H, Scott S M, Branch D W, Pluym T and Yarberry V 2013 On/Off Micro-electromechanical Switching of AlN Piezoelectric Resonators *Proc. IEEE MTT-S International Microwave Symposium* DOI: 10.1109/MWSYM.2013.6697719

[17] Yantchev V, Arapan L and Katardjiev I 2009 Micromachined Thin Film Plate Acoustic Wave Resonators (FPAR): Part II *IEEE Trans UFFC* **56** 2701-10

[18] Pluym T P, Choi S, Branch D W, Bauer T M, Stevens J E, Koch L F, Dyck C W, Nguyen J H, Sing M N, Scott S M, Olsson R H and Nordquist C D 2016 An Integrated Microresonator and Capacitive Switch Fabrication Process in preparation

[19] Branch D W, Wojciechowski K and Olsson R III 2014 Elucidating the origin of spurious modes in aluminum nitride microresonators using a 2-D finite-element model *IEEE Ultrasonics, Ferroelectrics and Frequency Control* **61** 729 – 38.

[20] Olsson R H, Nguyen J, Pluym T and Hietala V M 2014 A Method for Attenuating the Spurious Responses of Aluminum Nitride Micromechanical Filters *J. Microelectromech. Sys.* **23** 1198-207

[21] Nordquist C D and Olsson R H 2014 RF MEMS: Radio Frequency Microelectromechanical Systems *Wiley Encyclopedia of Electrical and Electronics Engineering* DOI: 10.1002/047134608X.W8229
[22] Olsson R H, Wojciechkowski K E, Tuck M R and Stevens J E 2009 Microresonant Impedance Transformers *Proc. IEEE Intl. Ultrasonics Symp* 2153-7.
[23] Bedair S S, Pulskamp J S, Polcawich R G, Morgan B, Martin J L and Power B 2013 Thin-Film Piezoelectric-on-Silicon Resonant Transformers *J. Microelectromech. Sys.* **22** 1383-94
[24] Song Y-H and Gong S 2015 Elimination of Spurious Modes in SH0 Lithium Niobate Laterally Vibrating Resonators *IEEE Elec. Dev. Lett.,* **36** 1198-1201
[25] Umeda K, Kawai H, Honda A, Akiyama M, Kato T and Fukura T 2013 Piezoelectric Properties of ScAlN Thin Films for Piezo-MEMS Devices *Proc. 2013 IEEE Intl. Conf. MEMS,* 733-736